Field enhancement effect of metal probe in evanescent field

Xiaogang Hong (洪小刚)[1], Wendong Xu (徐文东)[1*], Xiaogang Li (李小刚)[1]
Chengqiang Zhao (赵成强)[1], and Xiaodong Tang (唐晓东)[2]

[1] *Optical Storage Laboratory, Shanghai Institute of Optics and Fine Mechanics, Chinese Academy of Sciences, Shanghai 201800*
[2] *School of Information Science and Technology, East China Normal University, Shanghai 200241*
[*] *E-mail: xuwendong@siom.ac.cn*

Received May 5, 2008

Field enhancement effect of metal probe in evanescent field, induced by using a multi-layers structure for exciting surface plasmon resonance (SPR), is analyzed numerically by utilizing two-dimensional (2D) TM-wave finite difference time-domain (FDTD) method. In this letter, we used a fundamental mode Gaussian beam to induce evanescent field, and calculated the electric intensity. The results show that compared with the nonmetal probe, the metal probe has a larger field enhancement effect, and its scattering wave induced by field enhancement has a bigger decay coefficient. The field enhancement effect should conclude that the metal probe has an important application in nanolithography.

OCIS codes: 260.3910, 240.6680, 000.4430.
doi: 10.3788/COL20090701.0074.

Surface plasmon resonance (SPR) technology is developing rapidly in recent years. When a p-polarized light passes from a noble metal-coated prism to the interface between the prism and the metal film, a total internal reflection (TIR) takes place and an evanescent field comes into being. The incident photons are absorbed and the energy is transferred to the electrons. The electrons move in an evanescent wave way, which is called surface plasmons. The surface palsmons represent the electromagnetic surface waves that move along the interface, so it is called surface plasmon wave (SPW). SPR occurs when the momentum component of the incoming light along the interface is equal to that of SPW. The reflected light intensity decreases sharply and the electric field intensity of the evanescent field increases[1]. When SPR occurs, the angle of the incident light is called resonant angle (RA). Nowadays, SPR technology has been applied in various fields, including sensors, near-field scanning optical microscopy, thin film optics and thickness measurement, holography, precise measurement of angles, Q switching, and so on[2]. In addition, nanoscale metal structures, such as metal openings, metal tips, and metal particles, can excite localized SPR (LSPR) and result in localized field enhancement (FE) effect[3−5]. Because of this characteristic, SPR technology can be used in the field of Near-field microscopy[6−9] and nanolithography[10,11].

As we know, both the sensitivity and the resolution of Near-field microscopy and nanolithography are mainly determined by the probes used. At present, many papers have studied the characteristics of the metal-coated probe[12] or the metallic particle probe[13] which can not get the same effect as the metal probe. When the metal film coated is thick enough, the metal-coated probe can induce the same effect as the metal probe, but the radius of the tip will be too big to get a high resolution. Conversely, the nonmetal part of the metal-coated probe has effect because of the thin metal film. Although the metallic particle probe can achieve the same effect as the metal probe, it is not practical in nanolithography. In this letter, we mainly investigate the characteristics of metal probes, so that we can get an optimum probe for the potential nanolithography which uses a laser beam to induce Kretschmann SPR and utilize the metal probe's local-field enhancement effect to realize nanolithography.

This paper presents the main simulation results based on finite difference time-domain (FDTD) method which is a common way for calculating the electromagnetic field intensity. At first, we set the numerical model. Then we describe the SPR excited by a fundamental mode Gaussian beam with a wavelength of 514.5 nm. The FE effects of the metal and nonmetal probes are analyzed. The electric field intensity distributions on the surface of the photosensitive film are discussed. The decay coefficients of the scattering waves of the probes are also discussed. Finally we assess the possibility of the application of metal probe's FE effect in nanolithography.

The numerical model is shown in Fig. 1. This Kretschmann-type SPR structure contains five layers. It involves a transparent prism, a silver (Ag) film, a SiO_2 film, a photosensitive film (AgO_x), and a vacuum layer. Assume the incident angle as θ, and the RA as θ_R. The incident light electric field intensity is normalized. The Gaussian beam waist radius is 700 nm, and the waist is positioned at the interface between the prism and the silver film. The probe is cone shaped with a cone angle of 20°, and the tip is semicircular with a radius of 10 nm.

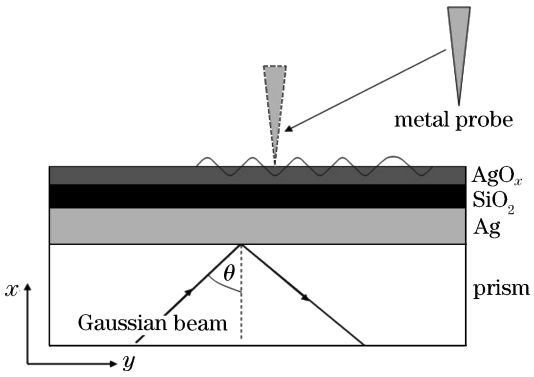

Fig. 1. Schematic diagram for the simulations.

Table 1. System Properties

Materials	Refractive Index /n (514.5 nm)	Film Thickness
Silver (Ag)	$0.130 + 3.051$j	40 nm
SiO_2	1.463	20 nm
AgO_x	$2.387 + 0.087$j	15 nm
Gold (Au)	$0.638 + 2.096$j	
Platinum (Pt)	$2.02 + 3.53$j	
Vacuum	1	
Prism (ZF6)	1.768	
Silicon (Si)	$4.225 + 0.06$j	
Silicon Nitride (Si_3N_4)	$2.212 + 0.0023$j	

Five kinds of probes will be simulated, including silver probe, gold (Au) probe, platinum (Pt) probe, silicon (Si) probe, and silicon nitride (Si_3N_4) probe. The system properties are shown in Table 1.

The model then implements the FDTD solution of the relevant scattered-field Maxwell equations. Specially, the Drude dispersion model[14] is used to simulate the metal film and metal probes, and the UPML absorbing boundary conditions are introduced. The simulation takes place in the specified region, which allows the complicated interaction of the incident beam with SPR structure and probes. So the required two-dimensional (2D) TM Gaussian beam can be produced. In the 2D FDTD solutions, the size of the cell is 2.5×2.5 (nm), and the number of the cells is 1500×4000.

One evident characteristic of SPR is that the reflected intensity of TIR decreases sharply when SPR occurs. And the reflectivity is equal to the square of the reflection coefficient of the electric field intensity[1]. With the normalized incident light electric field intensity, the reflected electric field intensity can describe SPR. A Kretschmann type SPR excited by a Gaussian beam is simulated. The electric field intensity of the reflected light varies as θ changes, as shown in Fig. 2, where the gray level expresses the electric field intensity. We can see that as θ changes from 45° to 60°, the reflected electric intensity decreases at first and reaches the valley at 51°, after that it increases on the contrary. So in this case θ_R is 51°.

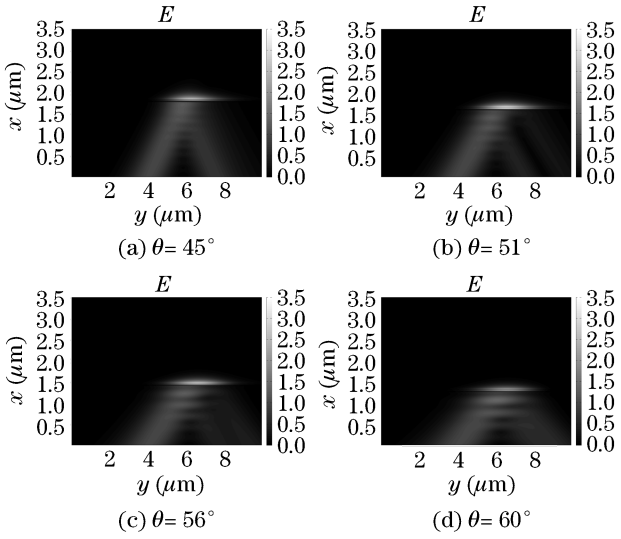

Fig. 2. Near-field intensity of electric field with different incident angle θ.

When SPR occurs, the energy of the incident light is held in the films and the electric field intensity of the evanescent field is enhanced. This is another significant characteristic of SPR, which is shown in Fig. 3. When the incident angle θ is equal to θ_R, the electric field intensity of the evanescent field reaches its maximum value. In this case, θ_R is 51°, and the maximal value of the electric intensity on the surface of the photosensitive film (EIMaxS) is 3.309. Scilicet the electric field intensity is enhanced by 3.309 times compared with the normalized incident light electric field intensity.

It is found that the evanescent field will influence the probes. We simulate the model with a probe in vacuum by changing the incident angle θ. And we set the coordinate of the point is (x_0, y_0) where the EIMaxS is. And the distance between the probe and the surface of the layers is 5 nm. So the probe is located at the point $(x_0 + 5, y_0)$, and the x coordinate of the surface of the photosensitive film is x_0.

The models were simulated with three kinds of probes. In Fig. 4, we can see that the curves of the electric field intensities of the models with probes at the point (x_0, y_0) on the surface of photosensitive of the film (EIS) on θ in Fig. 4(a) are similar to those in Fig. 3, and θ_R is hardly changes. The results show that the influence on SPR brought by the probe with a 10-nm radius tip can be ignored. Compared with the model with no probe, it can be concluded that the probe only changes the distribution of electric field intensity near it, as shown in Fig. 4(b). Figure 4(c) is the part near the probe of Fig. 4(b) where we can see that the probe can produce a spot with a diameter of twice of the radius of the tip.

As shown in Fig. 3, when the incident angle θ is not θ_R, the evanescent field is still enhanced. In order to describe the general characteristics of metal probe, we simulate the model in the case of $\theta = 56°$. The results are also suitable for θ_R.

Before a metal probe is introduced, the amplitude of the electric field intensity in the evanescent field can be expressed as

$$E_s(x_0 + x, y_0) = \mathrm{EIMaxS} \exp(-\alpha x), \quad (1)$$

where α is the decay coefficient and x is the distance between the surface of photosensitive film and the apex of the probe. When a metal probe is introduced, the electric field intensity at the apex $(x_0 + x, y_0)$ of the probe can be given by

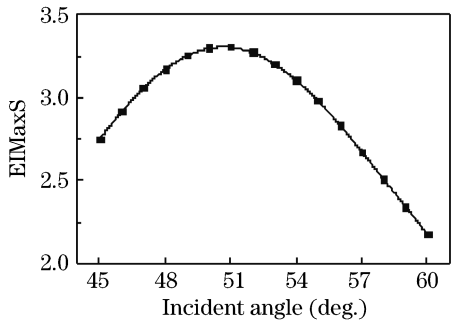

Fig. 3. EIMaxS of the model with probe on the incident angle.

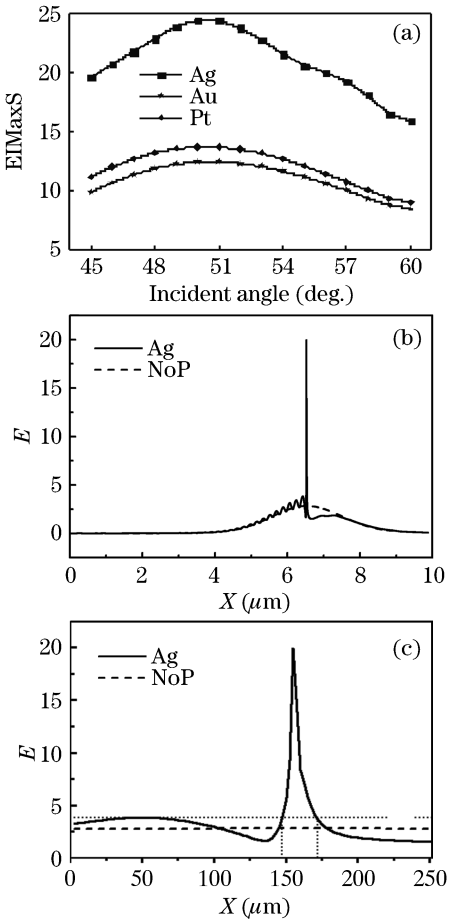

Fig. 4. (a) EIMaxS of the models with probes on the incident angle; (b) distribution of electric intensity on the surface of photosensitive film when $\theta = 56°$ (solid line for silver probe and dashed line for no probe); (c) the part near the probe of (b).

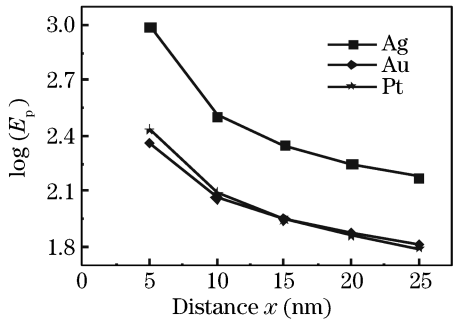

Fig. 5. Electric intensity at the apex of the metal probe versus the distance from the surface of the photosensitive film.

$$E_{\rm p} = GE_{\rm s}(x_0 + x, y_0) = G\text{EIMaxS}\exp(-\alpha x), \quad (2)$$

$$\log(E_{\rm p}) = \log(G\text{EIMaxS}) - \alpha x, \quad (3)$$

where G is the field enhancement factor of the probe.

The probe bring influence on the evanescent field, and the influence decreases as the distance increases. So when the distance is more than a certain value which in this paper is 10 nm, the influence brought by the probe can be ignored, and G becomes a constant, as shown in Fig. 5.

When a probe is introduced, EIS is determined by the electric field intensity of the evanescent field and the scattering field of the probe which is relative to the distance from the surface of the photosensitive film. As shown in Fig. 6(a), the scattering wave of the probe causes the exponential decay of EIS. So EIS can be given by

$$\text{EIS} = E_{\rm sm} + E_{\rm p}\exp(-\beta x), \quad (4)$$

where $E_{\rm sm}$ is the electric field intensity of the evanescent field positioned (x_0, y_0) when a probe is introduced, β is the decay coefficient of the scattering wave. Here $E_{\rm sm}$ can be substituted by the electric field intensity of the evanescent field with no probe $E_{\rm s}(x_0)$ with a low uncertainty $e(x)$ which decreases as x increases. Assuming that

$$\begin{aligned} -\beta x &= \log(\text{EIS} - E_{\rm sm}) - \log(E_{\rm p}) \\ &= \log(\text{EIS} - E_{\rm s}(x_0) - e(x)) - \log(E_{\rm p}) \\ &= \log(\text{EIS} - E_{\rm s}(x_0) - e'(x) - \log(E_{\rm p}), \end{aligned} \quad (5)$$

$$Z = -\beta x + e'(x) = \log(\text{EIS} - E_{\rm s}(x_0)) - \log(E_{\rm p}), \quad (6)$$

where $e'(x)$ given by $e(x)$ is also a low uncertainty. The curves of Z versus the distance x shown in Fig. 6(b) are almost straight lines. The decay coefficients of the scattering waves of different probes can be calculated, and the biggest is the one of gold probe. That is to say, the scattering waves of silver and platinum probes can propagate farther than those of the gold probe.

To show the metal probes' characteristics better, we simulated silicon and silicon nitride probes. The nonmetal probes can also enhance the field[10]. As shown in Fig. 7, the larger the refractive index, the greater the field enhancement. Because of the LSPR, the metal probe can obtain a greater enhancement than nonmetal, which is shown in Figs. 5 and 7, respectively.

Just like metal probes, nonmetal probes also scatter light energy. The obvious difference between them is that the scattering waves with the nonmetal probes have

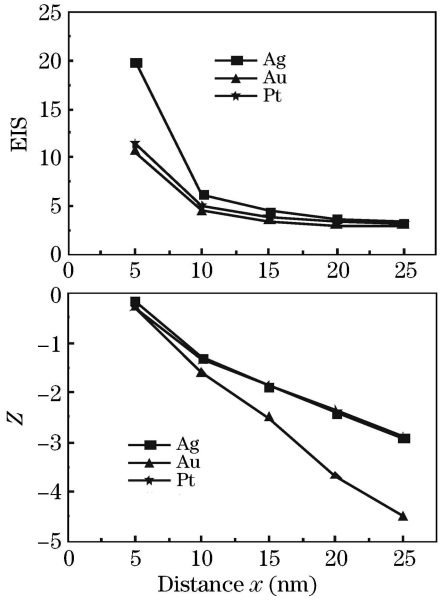

Fig. 6. (a) EISs of different metal probes plot and (b) Z of different metal probes plot.

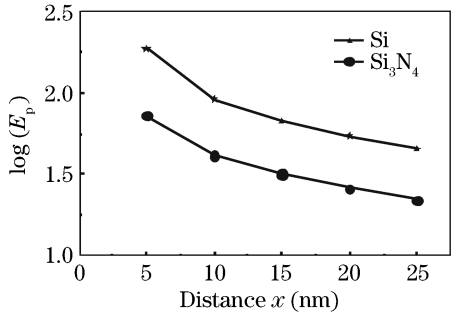

Fig. 7. Electric intensity at the apex of the nonmetal probe versus the distance from the surface of the photosensitive film.

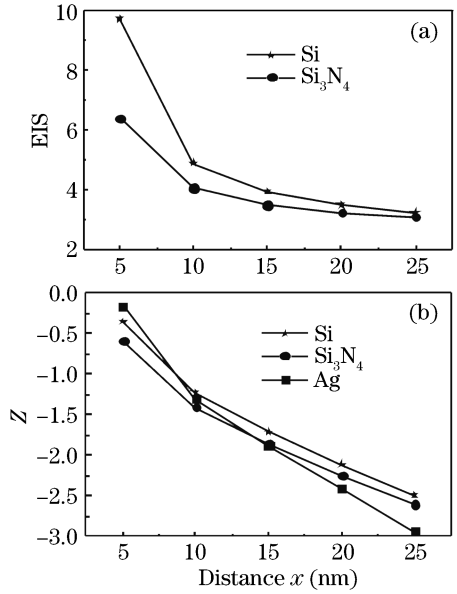

Fig. 8. (a) EIS of different nonmetal probes plot and (b) Z of different probes plot.

smaller decay coefficients, which result in longer propagation ranges than the metal probes. Assuming that the electric intensities at the apexes of the probes have the same values and the distances between the probes and the photosensitive films are equivalent, we can learn that the probe with small decay coefficient can pattern photosensitive film with deep marks.

In this letter, by using 2D TM-wave FDTD, we have carried out the simulation analyzing the characteristics of the metal probes in evanescent field, and satisfactory results are reached. At present, by using atom force microscopy (AFM) nonmetal probes and a Kretschmann type SPR structure, D. Haefliger and A. Stemmer[11] have written holes of 40-nm diameter and lines below 100-nm width into a 20-nm-thick aluminium film. Because of LSPR, the metal probes have greater field enhancement effects than those of nonmetal probes. For this characteristic, metal probe can be applied in the field of nanolithography and the needed incident power is reduced. Moreover, the metal probes' scattering waves possess bigger decay coefficients than those of the nonmetal probes. In summary, among Ag, Au, and Pt probes, Ag probe is suitable for nanolithography.

This work was supported by the Shanghai Committee of Science and Technology, China (No. 06DJ14007), the Major Program of the National Natural Science Foundation of China (No. 60490294), the National Natural Science Foundation of China (No. 50502036), and the "Dawn" Program of Shanghai Education Commission of China (No. 06SG30).

References

1. H. Raether, *Surface Plasmon on Smooth and Rough Surface and on Gratings* (Springer-Verlag, Berlin, 1988) p.13, p.16.
2. T. Zhang, M. Yi, Z. Fang, H. Yang, J. Yang, Y. Lu, H. Yang, H. Kang, and D. Yang, Physics (in Chinese) **34,** 909 (2005).
3. A. Hartschuh, M. R. Beversluis, A. Bouhelier, and L. Novotny, Phil. Trans. R. Soc. Lond. A **362,** 807 (2004).
4. Satoshi Kawata (Ed.), Motoichi Ohtsu, Masahiro Irie, *Near-Field Optics and Surface Plasmon Polaritons* (Spring-Verlag, Berlin, 2001) p.29.
5. J. Grand, M. Lamy de la Chapelle, J. L. Bijeon, P. M. Adam, A. Vial, and P. Royer, Phys. Rev. B **72,** 033407 (2005).
6. U. Ch. Fischer and D. W. Pohl, Phys. Rev. Lett. **62,** 458 (1989).
7. M. Specht, J. D. Pedarnig, W. M. Heckl, and T. W. Hänsch, Phys. Rev. Lett. **68,** 476 (1992).
8. S. I. Bozhvolnyi, I. I. Smolyaninov, and A. V. Zayats, Phys. Rev. B **51,** 17916 (1995).
9. I. I. Smolyaninov and David L. Mazzoni, Phys. Rev. B **56,** 1601 (1997).
10. Pascal Royer, Dominique Barchiesi, Gilles Lerondel, and Renaud Bachelot, Phil. Trans. R. Soc. Lond. A **362,** 821 (2004).
11. D. Haefliger and A. Stemmer, Ultramicroscopy **100,** 457 (2004).
12. W. Chen and Q. Zhan, Chin. Opt. Lett. **5,** 709 (2007).
13. G. Jian, F. Bai, S. Pan, and S. Wu, Acta Opt. Sin. (in Chinese) **25,** 470 (2005).
14. J. Tominaga and T. Nakano, *Optical Near-Field Recording: Science and Technology* (Springer-Verlag, Berlin, 2005) p.49.